Coexistence of magnetism and superconductivity in ultraclean underdoped $YBa_2Cu_3O_{6.37}$

R. I. Miller,[1] R. F. Kiefl,[1,2,3,*] J. H. Brewer,[1,2,3] F. D. Callaghan,[4] J. E. Sonier,[3,4] R. Liang,[1,3] D. A. Bonn,[1,3] and W. Hardy[1,3]
[1]*Department of Physics & Astronomy, University of British Columbia, 6224 Agricultural Road, Vancouver, British Columbia, Canada V6T 1Z1*
[2]*TRIUMF, 4004 Wesbrook Mall, University of British Columbia, Vancouver, British Columbia, Canada V6T 2A3*
[3]*Canadian Institute for Advanced Research—Superconductivity Program, Dundas Avenue, Toronto, Ontario, Canada*
[4]*Department of Physics, Simon Fraser University, Burnaby, British Columbia, Canada*
(Received 14 October 2005; published 11 April 2006)

Muon spin rotation and magnetization measurements in ultraclean single crystals of superconducting $YBa_2Cu_3O_{6+x}$ ($x=0.375$) reveal transitions at $T=19$ K to a bulk superconducting state and below $T=15$ K to a disordered antiferromagnetic state. The superconducting state pins magnetic flux. At the lowest temperatures an internal magnetic field with a magnitude close to that seen in the antiferromagnetic parent compound is present throughout the bulk of the sample. The two states coexist on a nanometer length scale, and over a narrow region of oxygen doping.

DOI: 10.1103/PhysRevB.73.144509 PACS number(s): 74.72.−h, 74.25.Ha, 75.40.−s, 76.75.+i

The close proximity of magnetic and superconducting phases is a common feature of all high-temperature superconductors and the interplay or competition between these ordered phases lies at the heart of the debate over the nature of these materials. The long-range antiferromagnetic order that is present in the parent compounds is destroyed by doping, but echoes of it are seen in the form of spin fluctuations observed far into the superconducting phase.[1] There is also considerable evidence that the superconducting phase is highly susceptible to the formation of static moments. For example, vortices formed by applying magnetic fields develop antiferromagnetism in their cores,[2,3] and magnetic moments seem to be induced by the presence of certain impurities such as Zn substituted for Cu.[4,5] Early muon spin rotation and relaxation (μSR) measurements on the first powdered $YBa_2Cu_3O_{6+x}$ cuprates[6–8] suggest that superconductivity coexists with static magnetic moments. Later measurements[9] on polycrystalline $YBa_2Cu_3O_{6+x}$ that has been doped with cations also show coexistence and a close agreement of the phase diagram with $La_{2-x}Sr_xCu_2O_4$. More recently, the heavily underdoped region of the phase diagram, where the superconductivity is weakest, has been explored[10] in polycrystalline samples with μSR. These recent results confirm the early measurements of Refs. 6–8 of the phase diagram, report a small area of overlap between superconductivity and a magnetic state, and establish that the antiferromagnetism and superconductivity occur in the entire sample very near the region of coexistence.

The meaning of this coexistence of magnetism and superconductivity is a central issue because it is not clear whether or not the static magnetic moments are secondary phenomena associated with the addition of defects and disorder, or a more general characteristic of the superconducting cuprates. In this paper we report on the presence of static moments that order at temperatures below $T=15$ K in single-crystal samples of $YBa_2Cu_3O_{6+x}$ ($x=0.375$). The ordering of the large magnetic moments occurs throughout the sample, despite the fact that this is a material doped without cation defects and has much weaker charge inhomogeneity than most cuprates. The fact that these samples also superconduct suggest that microscopic coexistence of superconductivity and magnetism is a stable feature in a very narrow part of the phase diagram even in the cleanest cuprate single crystals available.

The μSR measurements were performed at TRIUMF both in zero applied magnetic field (ZF μSR) with the muon polarization parallel (ZF_z μSR) and perpendicular (ZF_x μSR) to the $\hat{c}$ axis, and in an external magnetic field applied with the muon polarization perpendicular to the applied field ($\mu_0\vec{H}$) and the crystal $\hat{c}$ axis (TF μSR). Ultraclean $YBa_2Cu_3O_{6+x}$ single crystals used in this experiment were grown by a self-flux growth method in $BaZrO_3$ crucibles at the University of British Columbia. Precise control over oxygen concentration and overall oxygen homogeneity is required to produce the sharp superconducting transitions we observe with superconducting quantum interference device SQUID magnetometry (Fig.1). In $YBa_2Cu_3O_{6.375}$, the transition to a superconducting state occurs at $T_c=19$ K. The field-cooled magnetization is approximately 30% of perfect diamagnetism, similar to

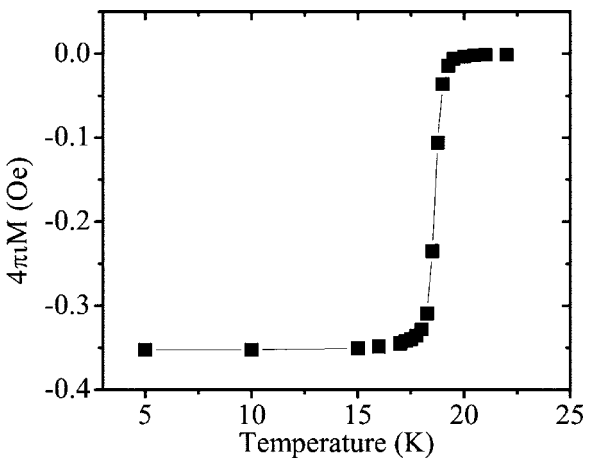

FIG. 1. Magnetization measurement in $YBa_2Cu_3O_{6.375}$ in an applied field ($H=1$ Oe) parallel to the $\hat{c}$ axis.

 ©2006 The American Physical Society

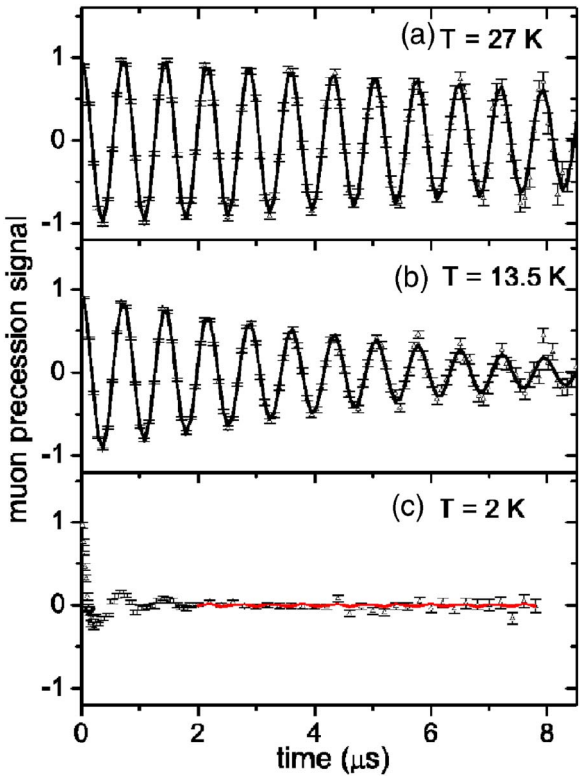

FIG. 2. (Color online) μSR signal in $YBa_2Cu_3O_{6.375}$ in an applied field $\mu_0 H(\|c)=100$ G in three distinct regions of the phase diagram. The applied field causes the μSR transverse field (TF) precession signal to oscillate at the Larmor frequency $\omega=\gamma_\mu H$ while spatial inhomogeneity in the magnetic field leads to a decay in the signal. (a) Nuclear moments lead to a slow decay of the signal at $T=27$ K. The data is fitted to a stretch exponential for comparison to (b). (b) TF μSR precession signal at $T=13.5$ K, below $T_c=19.5$ K. The increased damping [compared to (a)] below T_c is due to the presence of a vortex lattice. The data are fitted to a stretch exponential with parameters fixed to ZF data (see Fig. 3 below) multiplied by a Gaussian with a free damping parameter. (c) TF μSR precession signal at $T=2$ K. Here the rapid damping of the signal is dominated by spontaneous magnetic fields in the magnetically ordered state. The curve is a fit with a damped Gaussian to data at $t>2$ μs. The amplitude of the fitted signal is almost zero.

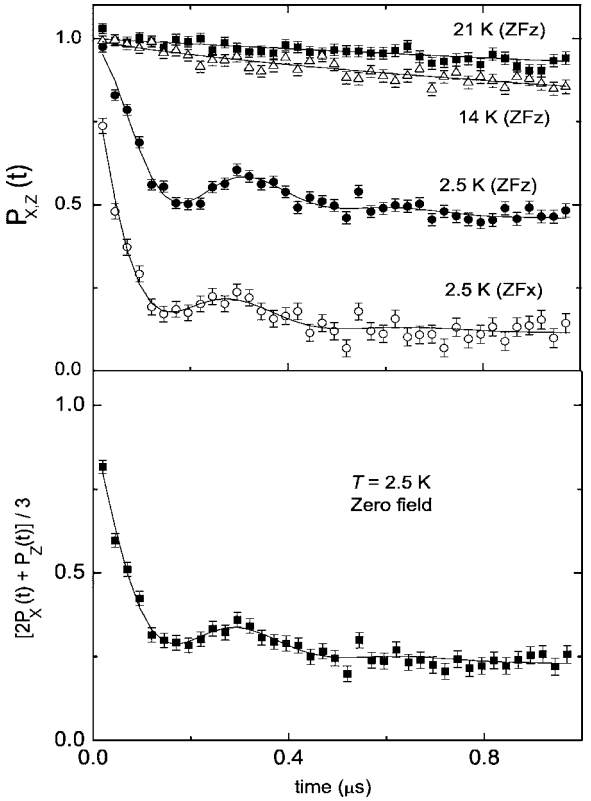

FIG. 3. (a) ZF μSR precession signals in $YBa_2Cu_3O_{6.375}$ with $P_\mu\|\hat{c}$ axis (ZF_z μSR) and perpendicular (ZF_x μSR). Both orientations of the spins reveal internal fields at $T=2.5$ K. (b) The composite spectrum $[2P_x(t)+P_z(t)]/3$ shows a 1/3 nonrelaxing component indicating that internal magnetic fields are present in all of the sample.

what is typically measured for optimally doped $YBa_2Cu_3O_{6+x}$. Such sharp transitions are particularly difficult to achieve because of the steep linear dependence of T_c on x (see solid squares in Fig. 6 below). Details on the growth method and crystal characterization can be found in Ref. 11.

In Fig. 2, we show the TF μSR precession signal in $YBa_2Cu_3O_{6.375}$ in three distinct regions of the phase diagram. In (a), the TF_x μSR precession signal at $T=27$ K is weakly damped due to small nuclear moments characteristic of the normal state in $YBa_2Cu_3O_{6+x}$ crystals. (b) shows the TF signal at $T=13.5$ K, which is below the critical temperature (T_c) measured by magnetization ($T_c=19$ K) but above the magnetic transition $T_M \approx 10$ K (see below). Here the sample shows an increased damping rate compared to (a) which as discussed below is partly due to the inhomogeneous field distribution present throughout the sample due to the vortex lattice. Finally, in (c) large spontaneous magnetic fields depolarize the signal rapidly at $T=2$ K, below T_M. Note that here the precession signal amplitude for $t>2$ μs is close to zero, implying that all muons see large local internal fields. A measurement at $T=2.5$ K of the ZF μSR precession signal (Fig. 3) reveals a broad distribution of spontaneous magnetic fields at the muon site, centered at 230 G. The rapid decay of the signal near $t=0$ μs indicates that the field distribution at the muon site is broad. Since the internal field in the parent compound is 300 G,[12] we conclude that the introduction of a small number of holes into the CuO_2 planes leads to a small but appreciable reduction in the density or magnitude of electronic moments. The presence of these large magnetic fields below T_M is what rapidly dampens the TF μSR precession signal shown in Fig. 2(c).

We have measured the volume fraction of the magnetic phase in this sample with ZF μSR. The ZF μSR precession can be measured with the muon spin both parallel and perpendicular to the $\hat{c}$ axis (see Fig. 3). The temperature dependence of the precession signal ($P_{\mu^+}\|\hat{c}\|\hat{z}$) shows a single-exponential behavior at $T=21$ K $>T_M$ with a relaxation due to Cu nuclear moments and an increase in the relaxation closer to T_M ($T=14$ K $\geqslant T_M$) due to a slowing down of the Cu electronic spins near the magnetic transition. At $T=2.5$ K, an oscillation is clearly visible near $t=0.3$ μs due to static internal fields in both orientations in Fig. 3. The aver-

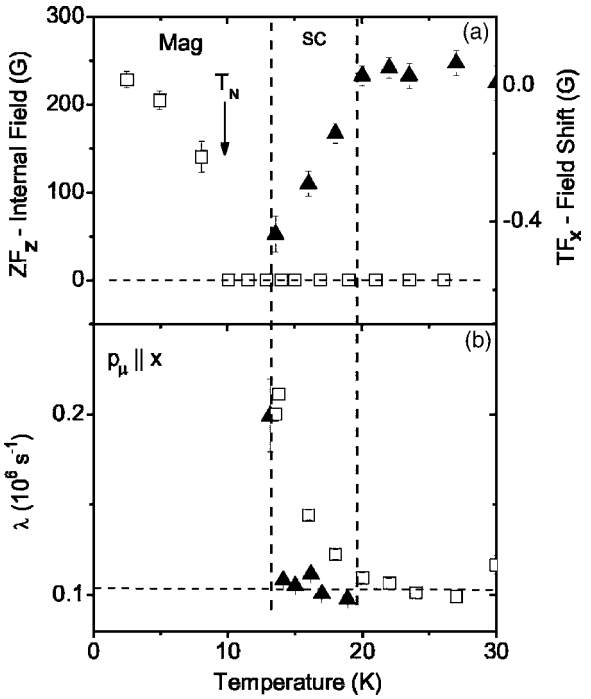

FIG. 4. (a) Internal field measured in ZF_z μSR (left axis, open squares). Diamagnetic shift of internal field $(\nu/\gamma_\mu - \mu_0 H)$ at muon site in an applied field $\mu_0 H(\|c) = 100$ G (right axis, filled triangles). (b) Relaxation rate measured in TF μSR σ_{TF} (open squares) and ZF μSR $\sigma_{ZF}/\sqrt{2}$ (filled triangles). The ZF relaxation rate above $T = 13.5$ K is due to Cu nuclear moments, while the Gaussian TF relaxation rate is caused by the vortex lattice that develops below T_c and the Cu nuclear moments. For $T \leqslant 13.5$ K, the electronic Cu spins add to the relaxation in both TF and ZF.

age field and width of the distribution of local fields determine the fast relaxing initial signal and oscillation. The differing longer time amplitudes of the ZF_x μSR and ZF_z μSR signals are due to the projection of the average local field at the muon site along the muon spin direction. The presence of the oscillations in both orientations show that the magnetic field at the muon site is neither along the $\hat{c}$ axis or in the ab plane, but must tilted at an angle from the $\hat{c}$ axis. Determining the orientation of the average local field requires higher statistics and more spectra with different orientations of the initial muon spin. The average internal field measured in these ZF spectra grows from zero above the transition to 230 G as $T \to 0$ K, shown in Fig. 4(a) and gives a transition temperature $T_M \approx 10$ K.

More importantly, the volume fraction of the magnetic phase can be extracted from a composite of the ZF_x and ZF_z precession spectra $(2P_x + P_z)/3$, which is shown in Fig. 3(b). This weighted sum simulates a powder average over internal field orientations. The long time polarization is $(26 \pm 3)\%$, near the expected 1/3 for a sample where the static fields are present in the entire sample. In particular, if a fraction of the sample were nonmagnetic and did not depolarize the muon precession, the long-time polarization would be larger than 1/3.

Below T_c but above the magnetic transition, the TF precession signal shows damping characteristic of a vortex lattice expected in the presence of an applied magnetic field [Fig. 2(b)]. The TF μSR polarization signal is given by $e^{-(\sigma_{TF}t)^2/2}\cos(2\pi\nu t + \delta)$. The damping parameter (σ_{TF}) models the relaxation from both the static Cu nuclear dipole moments and slowly fluctuating Cu magnetic moments and the relaxation due to the vortex lattice that occurs below T_c. The internal magnetic field at the muon site (ν) decreases at T_c as expected for a superconductor [Fig. 4(a)]. The ZF data are modeled with a Kubo-Toyabe function with damping parameter σ_{ZF} and $\sigma_{ZF}/\sqrt{2}$ is plotted in Fig. 4(b).[13] Above T_c the ZF relaxation rate follows the horizontal dashed line in Fig. 4(b). Below T_c it remains unchanged until $T \leqslant 13.5$ K, where the onset of the magnetic transition results in a large increase in σ_{ZF}. We have also applied a field (100 G) along the muon spin direction and measured σ_{ZF} (for $P_\mu \| \hat{z}$). A large decrease in the relaxation rate indicates that the local fields are primarily static on the muon time scale for $T > 13.5$ K.

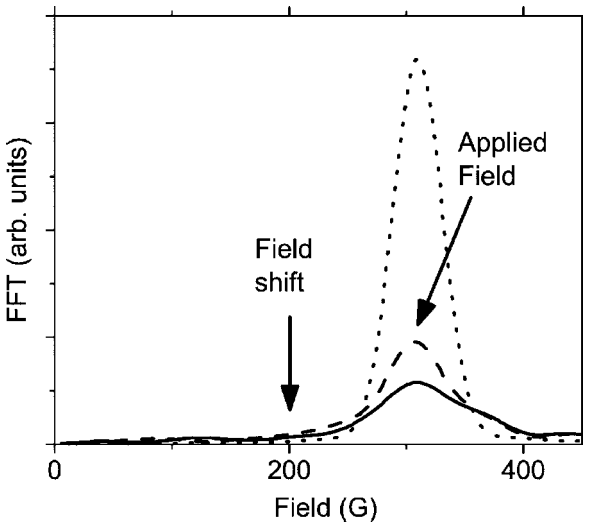

FIG. 5. Fast Fourier transform of the muon polarization signal in $YBa_2Cu_3O_{6+x}$ $x = 0.375$ in an applied field of 300 G at $T = 25$ K (dotted curve), $T = 3$ K (dashed), and $T = 3$ K (full) after shifting the applied field to 200 G.

At $T = 20$ K, $\sigma_{ZF}/\sqrt{2}$ and σ_{TF} are equal, but below T_c, the TF relaxation increases. This additional relaxation must be due to the presence of a vortex lattice and this conclusion does not depend on the exact form of the fitting function in ZF or TF. This TF relaxation establishes the bulk nature of the superconductivity in this highly underdoped $YBa_2Cu_3O_{6.375}$ sample because the relaxation is present in all the TF signal. A nonsuperconducting fraction of the sample would contribute a slower relaxing signal. These conclusions are in agreement with the results of Sanna *et al.* in polycrystalline samples.[10]

In order to further investigate the bulk nature of the superconductivity below T_c, we have also measured the TF μSR precession signal at low temperatures after shifting the applied field when at low temperature (Fig. 5). When a bulk superconductor is cooled in an applied field, pinning can trap magnetic flux in the sample. In such a case, when the applied field is changed while the sample is in the superconducting state (and below the depinning temperature), the TF signal

will continue to precess at the Larmor frequency corresponding to the applied field on cooling. We field-cooled the sample in an applied field of $\mu_0 H = 308$ G to $T = 3$ K and then decreased the applied field by 100 G. The μSR signal does not shift to 208 G, indicating that the low-temperature state can indeed pin the flux in the sample. In summary, we have shown that the sample exhibits a sharp superconducting transition at T_c, evidence of a flux lattice below T_c, and the ability to pin flux. Furthermore, a scanning Hall microscopy study on similar samples showed undistorted vortices at the surface.[14]

Together with the ZF results, these measurements show that at low temperatures single-crystal $YBa_2Cu_3O_{6.375}$ is both superconducting and magnetic. Chemical phase separation, where the oxygen concentration varies through the sample on a mesoscopic length scale (micrometers), can be ruled out by the sharp magnetization measurements and strong variation of T_c with small changes in x. Because the magnetic dipole field decays over about 20 Å and in $YBa_2Cu_3O_{6.375}$ all muons experience large magnetic fields of electronic origin in zero applied field, all muon sites must be within 20 Å of the static magnetism, as shown in Refs. 9 and 15. This observation excludes the kind of coexistence found in La_2CuO_{4+y},[15] where 40 Å islands occupy 40% of the sample. Thus charge and spin segregation occurs on a much finer scale in these $YBa_2Cu_3O_{6+x}$ samples, perhaps in the form of one-dimensional stripes, which have been widely reported in $YBa_2Cu_3O_{6+x}$ (Ref. 16) and $La_{2-x}Sr_xCuO_4$,[17], two-dimensional (2D) tightly packed nanometer islands of ordered spins (spin clusters), or a 2D grid of ordered spins randomly diluted by superconducting holes.

In $YBa_2Cu_3O_{6.365}$, there is a common transition to magnetism and superconductivity at $T_M = T_c = 14.5$ K,[18] and in $YBa_2Cu_3O_{6+x}$ samples with higher doping ($x = 0.53$, $T_c = 57$ K), we have previously reported that the magnetism in zero field is absent.[2] Thus, coexistence of antiferromagnetism and superconductivity in these single crystals occurs in a very narrow region of the phase diagram (Fig. 6) and these two states coexist throughout the sample on a nanometer length scale, in agreement with early[6] and more recent[10] studies of powdered $YBa_2Cu_3O_{6+x}$. Ideally, we would like to track the doping dependence of T_M for $0.38 < x < 0.53$; however, the chain oxygens do not order in this doping range and it is not yet possible to make ultraclean single crystals in this region with good oxygen ordering. Disorder caused either by cation doping or strain, often present in powder samples, is unlikely to cause the narrow region of coexistence in these single crystals, but may be responsible for the magnetism reported at higher doping in other cuprates.[1,9] It is possible that residual chain disorder plays a role in creating the narrow coexistence region we observe even in clean single crystals. However, the sharp superconducting transitions reported here suggests this is not the case and that there is a true, narrow region of coexistence near the antiferromagnetic-superconducting phase boundary, which is absent in most descriptions of the phase diagram.

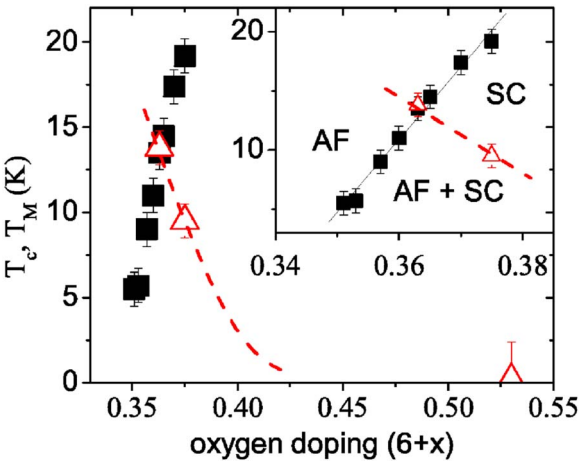

FIG. 6. (Color online) Phase diagram of $YBa_2Cu_3O_{6+x}$ from μSR measurements. The triangles (squares) are the magnetic (superconducting) transition temperatures. Below T_M, μSR observes static magnetism on the μSR time scale (MHz). T_c values are from Ref. 11 and this paper. In this area of the phase diagram, T_c increases very rapidly with oxygen content (x), while T_M decreases slowly as a function of x. In single crystals with $x = 0.53$, there is no evidence of a magnetic transition down to $T = 2.2$ K. Inset: expanded from main panel.

Technical help from M. Good, S. Kreitzman, B. Hitti, and D. Arseneau is acknowledged. R.I.M. thanks S. C. Zhang and G. Sawatzky for stimulating discussions.

*Electronic address: kiefl@triumf.ca

[1] C. Panagopoulos, J. L. Tallon, B. D. Rainford, T. Xiang, J. R. Cooper, and C. A. Scott, Phys. Rev. B **66**, 064501 (2002).
[2] R. I. Miller *et al.*, Phys. Rev. Lett. **88**, 137002 (2002).
[3] V. F. Mitrovic, E. E. Sigmund, M. Eschrig, H. N. Bachman, W. P. Halperin, A. P. Reyes, P. Kuhns, and W. G. Moulton, Nature (London) **413**, 501 (2001).
[4] P. Mendels *et al.*, Phys. Rev. B **49**, R10035 (1994).
[5] C. Panagopoulos, A. P. Petrovic, A. D. Hillier, J. L. Tallon, C. A. Scott, and B. D. Rainford, Phys. Rev. B **69**, 144510 (2004).
[6] J. H. Brewer *et al.*, Phys. Rev. Lett. **60**, 1073 (1988).
[7] J. H. Brewer *et al.*, Physica C **162**, 157 (1989).
[8] R. F. Kiefl *et al.*, Phys. Rev. Lett. **63**, 2136 (1989).
[9] C. Niedermayer, C. Bernhard, T. Blasius, A. Golnik, A. Moodenbaugh, and J. I. Budnick, Phys. Rev. Lett. **80**, 3843 (1998).
[10] S. Sanna, G. Allodi, G. Concas, A. D. Hillier, and R. De Renzi, Phys. Rev. Lett. **93**, 207001 (2004).
[11] R. Liang *et al.*, Physica B **383**, 1 (2002).
[12] N. Nishida *et al.*, Jpn. J. Appl. Phys., Part 1 **26**, L1856 (1987).
[13] In ZF, static local internal fields (B_i) in the plane normal to the muon spin relax the μSR signal. In TF, where $B_i \ll B_{ext}$, the TF relaxation is smaller by $1/\sqrt{2}$ because only fields along the external field will contribute to the dephasing and relaxation if they are static on the muon time scale. Because $\lambda_{ZF}/\sqrt{2} = \lambda_{TF}$ in our

measurements, most of the relaxation for $T > 13.5$ K must be due to static Cu nuclear dipolar fields.

[14] D. A. Bonn, J. C. Wynn, B. W. Gardner, Y. -J. Lin, R. Liang, W. N. Hardy, J. R. Kirtley, and K. A. Moler, Nature (London) **414**, 887 (2001).

[15] A. T. Savici *et al.*, Phys. Rev. B **66**, 014524 (2002).

[16] P. Dai, H. A. Mook, R. D. Hunt, and F. Dogan, Phys. Rev. B **63**, 054525 (2001).

[17] S. Wakimoto, R. J. Birgeneau, Y. S. Lee, and G. Shirane, Phys. Rev. B **63**, 172501 (2001).

[18] R. I. Miller *et al.* (unpublished).